Scott J.I. Walker, Anthony D. McDonald, Toshihiko Niki, Guglielmo S. Aglietti

DEVELOPMENT OF INFLATABLE STRUCTURES AT THE UNIVERSITY OF SOUTHAMPTON

University of Southampton
Southampton (UNITED KINGDOM)
sjiw@soton.ac.uk

Abstract

Inflatable technology for space applications is under continual development and advances in high strength fibres and rigidizable materials have pushed the limitations of these structures. This has lead to their application in deploying large-aperture antennas, reflectors and solar sails. However, many significant advantages can be achieved by combining inflatable structures with structural stiffeners such as tape springs. These advantages include control of the deployment path of the structure while it is inflating (a past weakness of inflatable structure designs), an increased stiffness of the structure once deployed and a reduction in the required inflation volume. Such structures have been previously constructed at the Jet Propulsion Laboratory focusing on large scale booms. However, due to the high efficiency of these designs they are also appealing to small satellite systems.

This article outlines ongoing research work performed at the University of Southampton into the field of small satellite hybrid inflatable structures. Inflatable booms have been constructed and combined with tape spring reinforcements to create simple hybrid structures. These structures have been subjected to bending tests and compared directly to an equivalent inflatable tube without tape spring reinforcement. This enables the stiffness benefits to be determined with respect to the added mass of the tape springs. The paper presents these results, which leads to an initial performance assessment of these structures.

1 Introduction

Inflatable technology has been used in aerospace applications over many decades as the ability to deploy large structures with a low mass and very high packing efficiency has always been a requirement in this industry. In fact some concepts were initially proposed as early as the 1930's. Two decades later, after the war years, various inflatable aircraft designs emerged from companies such as ML Aviation and Goodyear Aerospace and were subsequently constructed and flight tested with varying degrees of success [1]. These designs began the age of the inflatable aircraft. With recent advances in high strength fibers and rigidizable materials [2], inflatable technology has now matured into the space age as demonstrated by NASA's large-scale inflatable spacecraft 'TransHab' [3]. However, these structures are not only useful for large scale systems but may also be a very elegant solution for small scale deployment applications.

2 Small Satellite Applications

As a result of the research and development into the miniaturization of electronic and mechanical technologies, satellites can now be constructed with a much lower mass reducing the overall mission cost. However, despite this mass reduction, the requirement to deploy areas larger than the satellite surface remains. These deployed areas are used in applications such as power arrays, antennae, de-orbit devices and in some cases solar sails [4], [5]. The miniaturization of larger deployment systems does not result in efficient designs due to the complexity of mechanisms and electric motors. In order to produce efficient and reliable small satellite deployable structures more novel technologies are required. These applications, amongst others, have driven the development of inflatable technologies for space missions and have led to many exciting development concepts.

Since the 1980's a significant amount of research has been performed studying various configurations of inflatable booms as both stand alone components

and parts of area deployment devices and antennae [6]. In recent years this work has been led by the Jet Propulsion Laboratory (JPL) in conjunction with two specialist companies, L'Garde and ILC Dover based in the USA [7]. Various specifics of the inflatable booms have been investigated to identify the best materials for space applications and potential weaknesses of these structures. It was concluded that they are most structurally efficient when combined with metal stiffeners known as tape springs [6]. Tape springs (defined as thin metallic strips with an initially curved cross section) have already been investigated in the space industry as hinges/hinge components by many companies (Surrey Satellite Technology Limited [8], Metravib [9], etc). However, the combination of inflatable material and tape springs creates a hybrid structure that has a superior performance when compared to the individual components. The tape springs help to guide the deployment and prevent localised compression when the structure is subjected to a load and the inflatable structure increases the booms second moment of area by distancing the tape springs from the neutral axis. Examples of these structures have been built by JPL that have a diameter of 0.076m and a length of 5m. Further work is underway to develop this technology for larger deployments as required by the American space industry [6]. However, they have not been investigated and optimized for small satellite applications with more limited financial budgets, more common in the UK and European market. The aim of this work is to study these small scale hybrid structures in more depth, focusing on their deflection under an applied load, to identify the stiffness benefit with respect to the added mass penalty.

3 Experimental Development and Material Testing

Modern inflatable structures for aerospace applications are mostly constructed from advanced fibers such as Vectran and Kevlar along with more conventional fibers such as Nylon [6]. These fabrics have been used with coatings such as polyurethane and provide the main structural resistance to the internal inflation pressure. The main air tight seal is provided by an internal bladder made from materials such as polyurethane. Rigidization of the inflated booms can be achieved by using specific fabric coatings or through the use of specialized materials such as aluminium laminate [6]. However, rigidization methods are beyond the scope of this initial research.

Through initial investigations into sourcing these modern fabrics it was found to be very costly to purchase the small amounts of the materials required for this initial research effort. Alternate materials were sourced that are more widely used in terrestrial applications such as sailing. These materials ranged from coated or impregnated Ripstop Nylon and Ripstop Polyester. Nylon and Polyester are both fibers that have been used previously in aerospace inflatable applications [6], [1]. When using fabrics as a structural material it is important to understand the properties of the materials which directly relates back to its method of construction. The synthetic man made fibres are initially formed into yarn so it can woven together to make the fabric. The weaving process incorporates longitudinal yarn running along the length of the fabric roll and transverse yarns which are weaved into the longitudinal yarns to create the roll of fabric. The directions of the longitudinal and transverse yarns are known as the warp and fill directions respectively. Typically the material properties vary between the warp and fill orientations and more significantly in the bias direction which is 45^o in between the warp and fill directions. In this respect these properties are similar to 0^o, 90^o composite laminates.

The initial aim was to test an inflatable tube with a radius of 50mm, up to an inflation pressure of 103.4N/m^2 (15psig). For initial calculation purposes if a material thickness of 0.1mm is assumed, an initial estimate into the required hoop stress (σ_H) of the material can be calculated. For this geometry, at this pressure the selected material must be able to withstand a hoop stress of 51.7MPa. Along with the strength requirement the fabrics also need to have the ability of maintaining the required shape when inflated (i.e. avoid 'ballooning'). A range of more than 20 fabrics were obtained and tested in Instron machines using two test samples per fabric to determine the tensile strength and Young's modulus of the samples in the warp direction. This allowed an initial material selection based on ultimate tensile strength, mass and availability before more in-depth testing was performed. Initial inflation tests of small tubes were also per-

formed to identify the materials that were susceptible to ballooning, allowing the most suitable fabric to be selected. This resulted in the selection of 'Fibermax 94'. Fibermax is an advanced sailcloth fabric that is constructed with the maximum number of nylon fibres which is then dipped through a solution of dissolved resin. The resin is cured at a high temperature resulting in very small resin particles being embedded in the weave, restricting its stretch [10]. From the material tests it proved to be one of the optimum fabrics in terms of the strength to mass ratio. This selected material was subsequently tested repeatedly in the Instron machines in both the warp and fill directions to more accurately determine the material properties. Five further samples were tested in the warp direction and five samples were tested in the fill direction. Each sample was cut into 50 x 200mm strips which when clamped resulted in a test length of 100mm. The samples were extended at a rate of 5mm per minute in an Instron machine until destruction as shown in Fig. 1. The results for all seven tests in the warp direction are displayed in Fig. 2 and the five fill direction test results are shown in Fig. 3. It

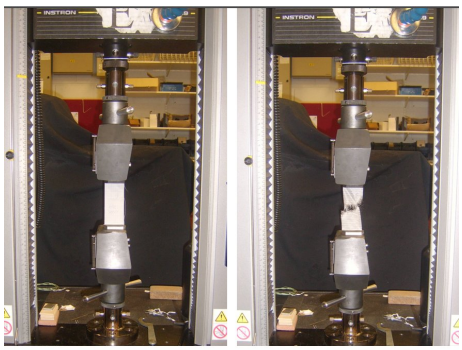

Figure 1: Fabric material testing using an Instron machine

can be seen from Fig. 2 that the stress-strain relationship for the warp direction is non-linear, which is common for fabrics due to the weave construction [11]. Various gradients could be used to determine a value of the Young's modulus, the simplest being the gradient between the zero stress point and the point of failure. For the data shown in Fig. 2 this simple approach to determine the Young's modulus produces values ranging from 0.22GPa to 0.29GPa, with a mean average value of 0.28GPa. The equivalent average Young's modulus for the fill direction is

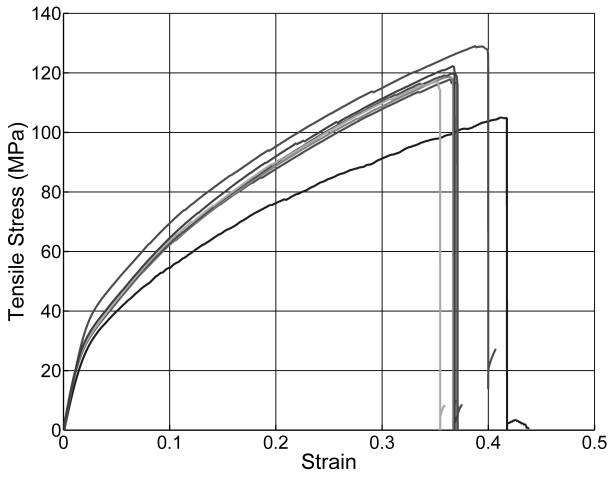

Figure 2: Stress/strain properties for Fibermax94 in the warp direction

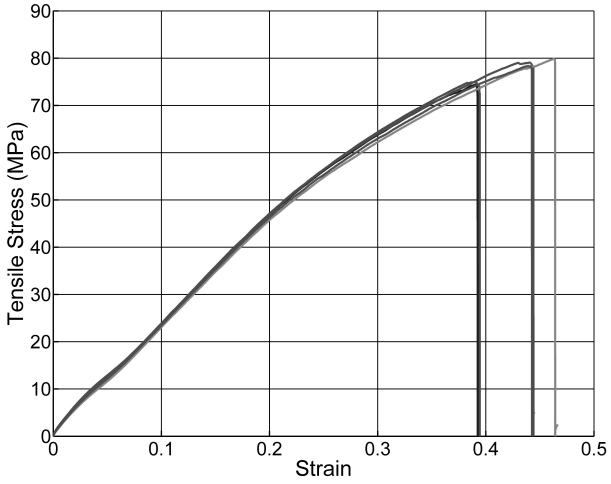

Figure 3: Stress/strain properties for Fibermax94 in the fill direction

0.188GPa. The average ultimate tensile stresses for the warp and fill directions are 119MPa and 77MPa respectively. To identify the potential variability in the gradient the warp direction curve can be analysed over different strain regions giving a complete gradient range from 0.125GPa to 1.6GPa. If the anticipated stress/strain is low then a higher Young's Modulus value should be used. For higher levels of strain a function should ideally be used to model this relationship. However, permanent deformation strain in the material would alter this function, so careful material testing is required. These complexities are beyond the scope of this initial study but are currently under investigation.

The magnitude of stress/strain experienced by the fabric is dependant on the material used for the

bladder. The choice of material for the inner bladder was limited by the properties required of it, i.e. being non-permeable and able to expand to the internal shape of the tube. An ideal material that met these requirements and that was freely available was latex rubber. Two thicknesses were initially tested and the lower thickness of 0.5mm was finally selected due to its expansion properties. Five samples were tested in the intron machine using the same sample size as previously described. The results are shown in Fig. 4. It can be seen that

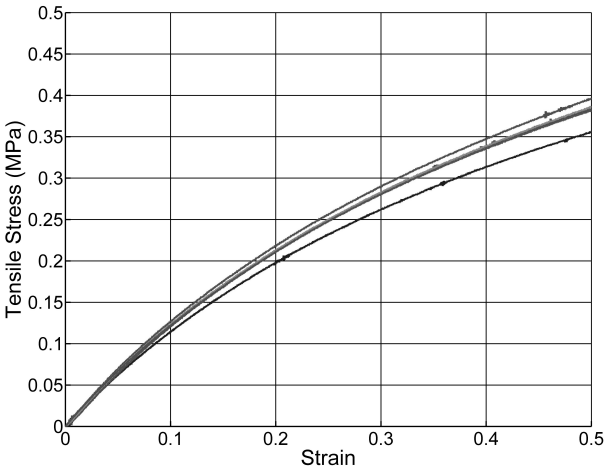

Figure 4: Stress/strain properties for latex rubber

the rubber easily expands allowing the majority of the inflation stresses to be taken by the outer fabric as required.

4 Experimental Testing

In order to investigate the deflection of hybrid structures, inflatable tubes were constructed with a radius of 50mm. This dimension allows easy access to internal seams but also minimises the size of the supporting structure. The fabric tubes were constructed from two fabric areas, one creating the circular end and the other the longitudinal tube. These were sewn together using a simple stitch with one seam running along the length of the tube. The inner bladder was constructed using the same material pattern. However the seams were bonded using a water based adhesive called Copydex.
The test campaign focused on determining the tip deflection of a cantilevered inflatable tube subjected to a tip load. Three test variables were analysed, namely: tube length, inflation pressure and section configuration. Three tube lengths of 0.6, 0.4 and 0.2m were each tested at two inflation pressures of 68.95kNm^{-2} and 103.4kNm^{-2} (10 and 15psig respectively). Four section configurations were tested to identify the stiffening effect of various permutations of tape springs. These configurations were:

- an inflatable tube with no tape spring stiffeners
- an inflatable tube with one pair of small tape springs
- an inflatable tube with one pair of large tape springs
- an inflatable tube with two large tape spring pairs.

The section configurations are shown graphically in Fig. 5 along with the direction of the applied load (F). The three parameters that define the

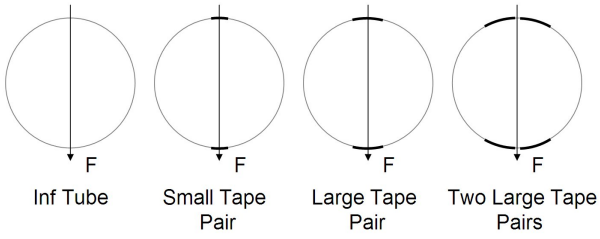

Figure 5: Section configurations shown with applied load, F

section geometry of a tape spring are: radius of curvature, R, angle of embrace, α and thickness, t. These properties are shown graphically in Fig. 6 and are listed in table 1 for the tapes springs tested. The tapes springs are made of steel with the standard material properties. The hybrid

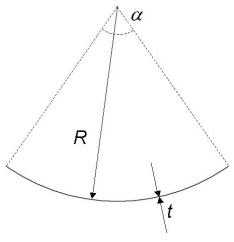

Figure 6: Cross sectional tape spring parameters

tubes were mounted at the root end to form a cantilever beam. The root mounting was achieved with

Section Parameter	Small Tape Spring	Large Tape Spring
$R\ (mm)$	14.7	14.5
$\alpha\ (rad)$	0.912	1.83
$t\ (mm)$	0.145	0.162

Table 1: Parameters of Tape Spring Sections

two base plates, one inside and one outside the material layers which when screwed together created the air tight seal. A further thin metal plate (with a mass of 46g) was inserted at the tip between the fabric layer and the bladder to spread the applied tip load across the section. This also formed a solid reference point for deflection measurements. The tip loads were applied using suspended weights mounted at the centre of the fabric end area. Deflection measurements were taken with a height gauge which could measure displacements up to 300mm with an accuracy of 0.01mm. This experimental configuration is shown in Fig. 7. As many different section configurations were

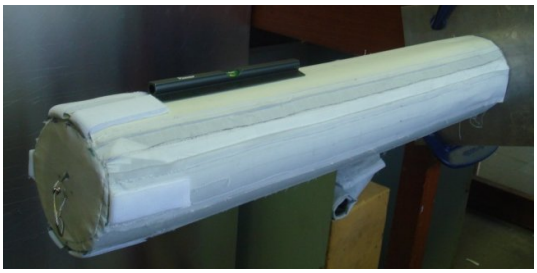

Figure 7: Experimental configuration shown with spirit level

to be tested, the fabric tubes were designed with sewn pockets running along the length of the tube allowing both sizes of tape springs to be inserted and removed as required. The longitudinal movement of the tape springs relative to the fabric was prevented by using velco flaps at the end of the pockets. Eight pockets were arranged around the circumference as displayed in Fig. 8, four for each tape spring size. The tube was rotated and remounted to achieve the required loading cases as shown previously in Fig. 5. Five repeat deflection tests were performed for each test permutation resulting in a total number of 120 deflection tests. As the tape springs were attached to the tube using the fabric pockets, the tape spring root end did not attach rigidly into the root mounting. However tape spring roots were supported using the outer circumference of the inner root plate, which after buckling resulted in permanent deformation to the tape spring steel. The tape springs therefore required replacement after every deflection test to failure. Although the tape spring root attachment was not ideal, it was acceptable for the initial tests due to the large number of test permutations required.

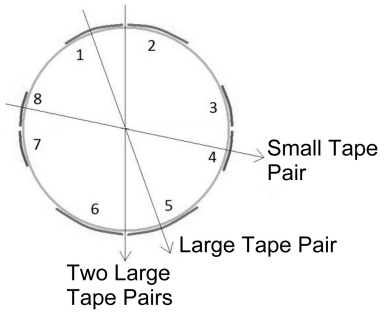

Figure 8: Tape spring mounting/pocket locations and loading directions

At the start of each displacement test the tube was mounted horizontally, checked with a spirit level and the initial tip height was noted. Initially the hook supporting the weights (of mass 0.5kg) was attached and the tip displacement recorded before each weight was added in increments of 1kg. The tip displacement was recorded after each force increment up to either an excessive displacement after buckling, or the total added mass of 12.5kg being reached. The mass of each configuration is shown in table 2.

	Mass (g) for length		
Configuration	0.6m	0.4m	0.2m
Inf Tube	210	163	115
Small Tape Pair	222	171	119.2
Large Tape Pair	236	179.6	123.4
Two Large Tape Pairs	262	196.2	131.8

Table 2: Configuration masses

5 Experimental Results and Discussion

Due to the large quantity of deflection tests performed it is first necessary to determine if the average deflections (over the five repeat tests for each

configuration) are representative of the data. The average deflection curves could then subseqently be used for data comparisons. All the individual deflection test results are displayed in Fig. 9, Fig. 10 and Fig. 11 along with the averaged result for each tube length and pressure. Although these graphs are densely populated they are only used at this stage to show the applicability of the average result and to identify basic trends. The deflec-

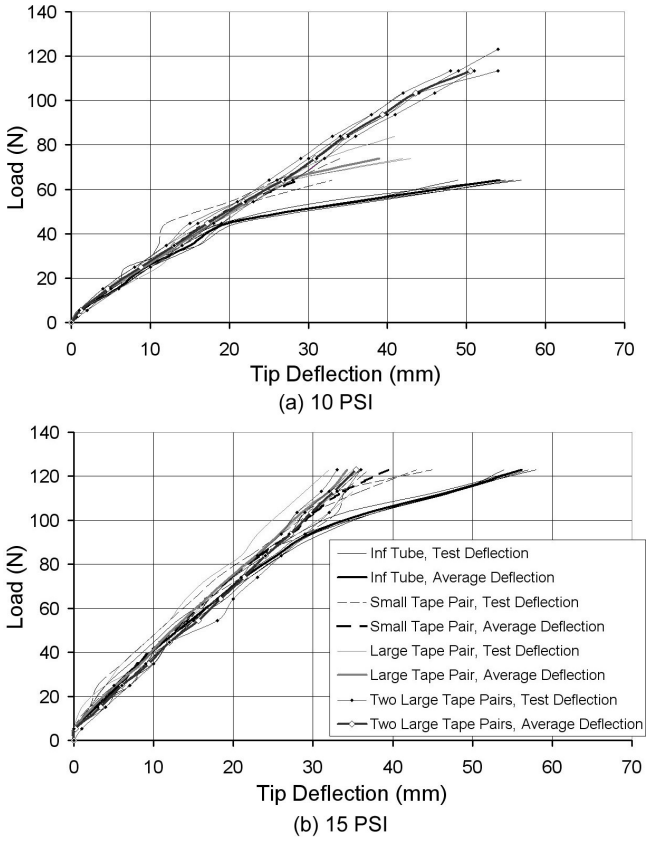

Figure 9: Tip deflection displacement for 20cm tube

tion data for the 0.2m tube is shown in Fig. 9. From the deflection data for an inflation pressure of 68.95kNm^{-2} (10 PSI), Fig. 9(a), the first noticable trend is the linearity of the data, displaying a clear stiffness relationship between applied load and deflection. It can also be seen that athough there is variability in the data, the averages are a good representation of the trends. Some inaccurate individual data points can be identified, but these do not heavily influence the average result due to the number of repeat tests performed. The effect of the tape spring stiffeners is clearly displayed in this figure. The structure becomes significantly

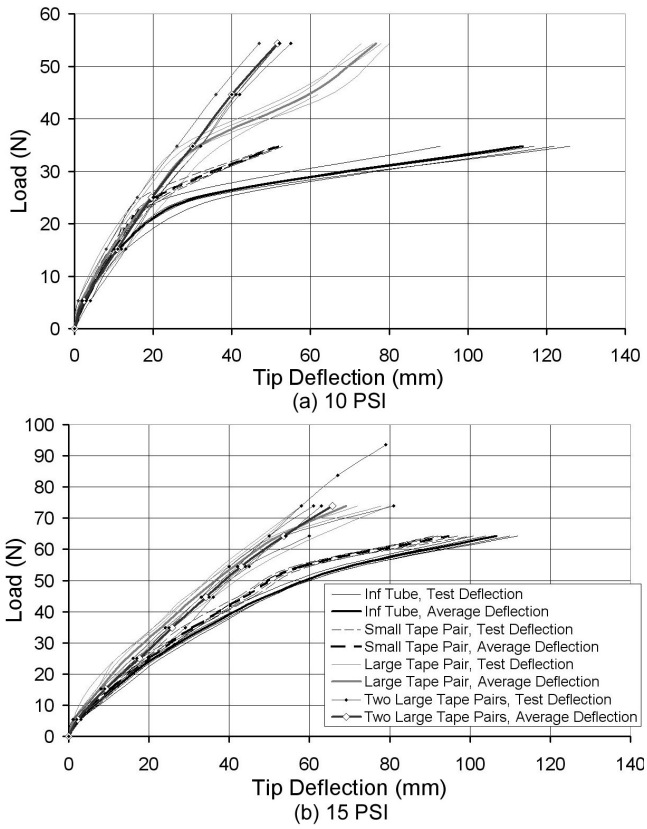

Figure 10: Tip deflection displacement for 40cm tube

more able to resist buckling. Similar trends can be seen for the 0.2m tube at the higher pressure of 103.4kNm^{-2} (15 PSI), Fig. 9(b). However for this case the stiffness gradient has increased due to the higher pressure, and the inflable tube's ability to resist buckling has increased as a result. Therefore the benefit of the structural stiffeners becomes less apparent. The deflection data for the 0.4m tube is shown in Fig. 10. The results for the lower pressure (Fig. 10(a)) displays a very clear repeat of the trends found in Fig. 9(a). The buckling point of each structural configuration is clearly represented along with the applicability of the average result. At the higher pressure the inflatable tube is more resistant to buckling but the stiffness relationship for the weaker two configurations is less than that displayed by the stiffer configurations. As a result, no clear buckling point can be identified for the inflatable tube configuration. Fig. 11 shows the equivalent deflection data for the 0.6m tube and displays similar data trends. However due to the increased length of the tube, the buckling loads of the inflatable tube configuration become more de-

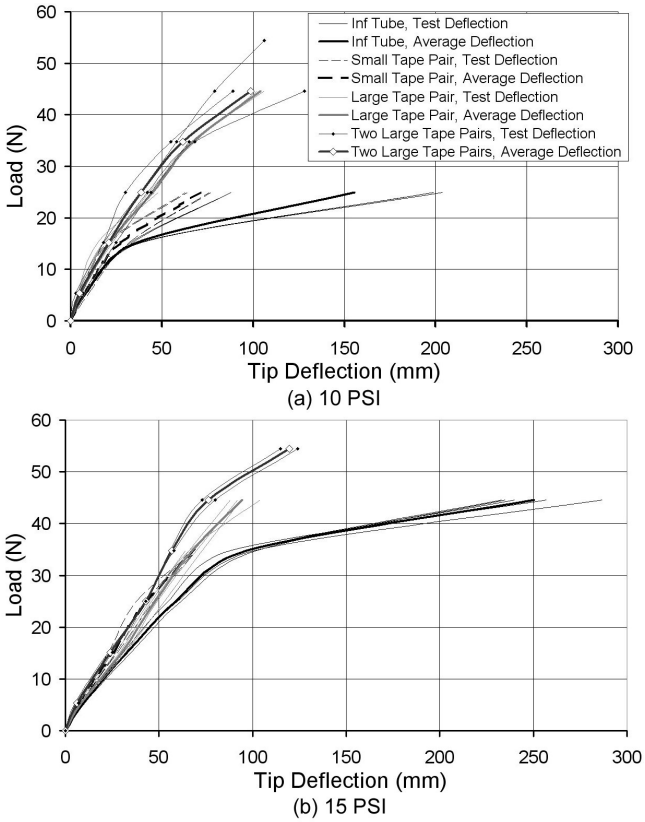

Figure 11: Tip deflection displacement for 60cm tube

fined. A clear buckling point can now be identified for the stiffest configuration as displayed in Fig. 11(b).

In order to analyse the data equivalently for all tube lengths the root bending moment can be determined for each case and plotted against the tip deflection. This allows the root bending moment magnitude that causes the buckling failure to be determined. Fig. 12 displays the average tip deflection data with respect to the applied root bending moment for the inflatable tube configuration. It can be seen from this data that, as bending theory suggests, the bending moment to cause a buckling failure is independant of tube length and is more or less consistent for each inflation pressure. The exact magnitude that defines the onset of buckling is somewhat subjective, but it is around 8Nm and 19Nm for 10PSI and 15PSI respectively. These values can now be used to assess the performance benefits of using the tape spring structural stiffeners.

Fig. 13 shows these average inflatable tube tip deflection results along with the other configuration tip deflection averages at a pressure of 10PSI.

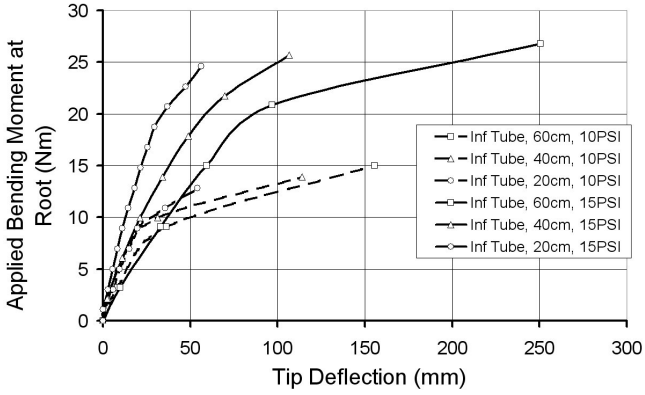

Figure 12: Applied root bending moment against tip deflection for the inflatable tube configuration

By studying the small tape pair deflection data it can be seen that the onset of buckling occurs at a root bending moment magnitude of between 8 and 10Nm. The 0.6m displacement result for this configuration shows a relatively smooth curve, whereas the shorter lengths show a more defined transition between 9 and 10Nm. A figure of 9Nm will therefore be used as a conservative estimate for this configuration. For the third configuration, the long tube length displacement result is not linear, and hence cannot be used with any certainty as to the point of buckling. However the shorter tube lengths both display a clear gradient change between 13 and 14Nm, resulting in a conservative value of 13Nm for further analysis. The fourth configuration again displays a smoother gradient change for the long tube length, making a single buckling point hard to determine. The shorter lengths suggest a value of around 20Nm.

The equivalent data for the higher inflation pressure is shown in Fig. 14. As with the lower inflation pressure deflection data the longer tube lengths are inclusive when attempting to determine the buckling root moment for the small and large tape pairs. However for the small tape pair the maximum bending moment applied to the long tape length was 21Nm. This value is around the onset of buckling for this configuration as shown by the shorter tube lengths. The point of buckling for the stiffer two configurations at this higher pressure are harder to assess as the maximum tip force does not exceed the buckling moment for the shorter lengths. However, using the longer lengths it can be concluded that the root bending moment for failure, for these two configurations is not less than 25Nm.

These root bending moment magnitudes that result in a buckling failure are summarised in table 3.

Configuration	Root bending moment for buckling failure (% change with respect to *) 10 PSI	15 PSI
Inf Tube	8*	19 (137.5)
Small Tape Pair	9 (12.5)	21
Large Tape Pair	13 (62.5)	25
Two Large Tape Pairs	20 (150)	25

Table 3: Root bending moment for failure comparision

By studying the mass data shown previously in table 2 it can be seen that the mass of the inflatable tube without stiffeners can be modeled as a function of length using equation 1, where the mass and length is measured in grams and metres respectively.

$$Mass_{tube} = 237.5 \times length + 67.7 \qquad (1)$$

This function enables the mass of the tube, which changes with length, and the mass of the end cap to be determined. If the tapes spring masses per unit length are known to be 10g/m and 21g/m for the small and large tapes respectively then these values can be ratioed with the length variable of the tube mass to determine a percentage mass increase which is independant of length. This results in the percentage mass increases shown in table 4. These

Configuration	% mass increase of tube length
Small Tape Pair	8.4
Large Tape Pair	17.7
Two Large Tape Pairs	35.4

Table 4: Percentage mass increase of inflatable tube

values can be compared with the root bending moment for failure values shown in table 3 which are also independant of tube length.
From the data shown it is known that increasing the structural stiffening in the tube increases the tubes ability to resist buckling. However we can use the data displayed in table 3 to initially quantify this effect and to offset this benefit with the mass increase shown in table 4. By adding small tape springs into the structure we have gained a strength increase of 12.5% at a mass increase of 8.4%. As these numbers are only approximate figures we can state that for small stiffeners the strength and mass increases are almost comparable. As more stiffeners are applied to the structure, the system becomes more efficient, with the percentage stiffness increase rising faster than the mass percentage. However, the stiffness increase for the two large tape pair configurations is now comparable to an increase in internal pressure to 15PSI. This was achieved with a mass increase of about 35%. The use of tape spring stiffeners therefore becomes a trade off between the mass increase of the tape spring stiffeners and the mass increase required to provide and sustain an equivalent higher pressure system.

6 Conclusions

This paper has outlined ongoing work at the University of Southampton into the field of hybrid inflatable structures for small satellites. Some experimental methods and results have been presented allowing initial performance estimates to be determined. The structural benefits and mass penalties have been roughly quantified enabling an initial comparison of higher pressure systems and hybrid structures. It can be concluded that both approaches are effective at increasing the boom stiffness and the optimum structure is dependant on the mass required to achieve and sustain the higher pressure system.

References

[1] Cadogan, D., Smith, T., Lee, R., Scarborough, S., and Graziosi, D., "Inflatable and rigidizable wing components for unmanned aerial vehicles," 2003, pp. 3688–3695, Apr 7-10, Norfolk, VA, United States.

[2] Scarborough, S. and Cadogan, D., "Rigidizable materials for inflatable space and terrestrial structures," 2005, May 1-5, Long Beach, CA, USA.

[3] de la Fuente, H., Raboin, J., Spexarth, G., and Valle, G., "TransHab: NASA's large-scale

inflatable spacecraft," 2000, Apr 3-6, Atlanta, GA, USA.

[4] Derbes, B., "Case Studies in Inflatable Rigidizable Structural Concepts for Space Power," 1999, Jan. 11-14, Reno, NV, AIAA-99-1089.

[5] Derbes, B., Veal, G., Rogan, J., and Chafer, C., "Team Encounter Solar Sails," 2004, Apr. 19-22, Palm Springs, California, AIAA-2004-1577.

[6] Lou, M., Fang, H., and Hsia, L., "A Combined Analytical and Experimental Study on Space Inflatable Booms," Vol. 2, 2000, pp. 503–512.

[7] Huang, J., "The Development of Inflatable Array Antennas," *IEEE Antennas and Propagation Magazine*, Vol. 43, No. 4, 2001, pp. 44–50.

[8] Walker, S. and Aglietti, G., "Modeling the Hinge Moment of Skew Mounted Tape Spring Folds," *Journal of Aerospace Engineering*, Vol. 20, No. 2, 2007, pp. 102–115.

[9] Givois, D., Sicre, J., and Mazoyer, T., "A Low Cost Hinge for Appendices Deployment: Design, Test and Applications," *9th European Space Mechanisms and Tribology Symposium ESA/ESTEC*, 2001.

[10] "Fibermax Stabilized Nylon," *Challenge Sailcloth Sales Brochure*, 2009.

[11] Firt, V., *Statics, Formfinding and Dynamics of Air Supported Membrane Structures*, Martinus Nijhoff Publishers, 1983.

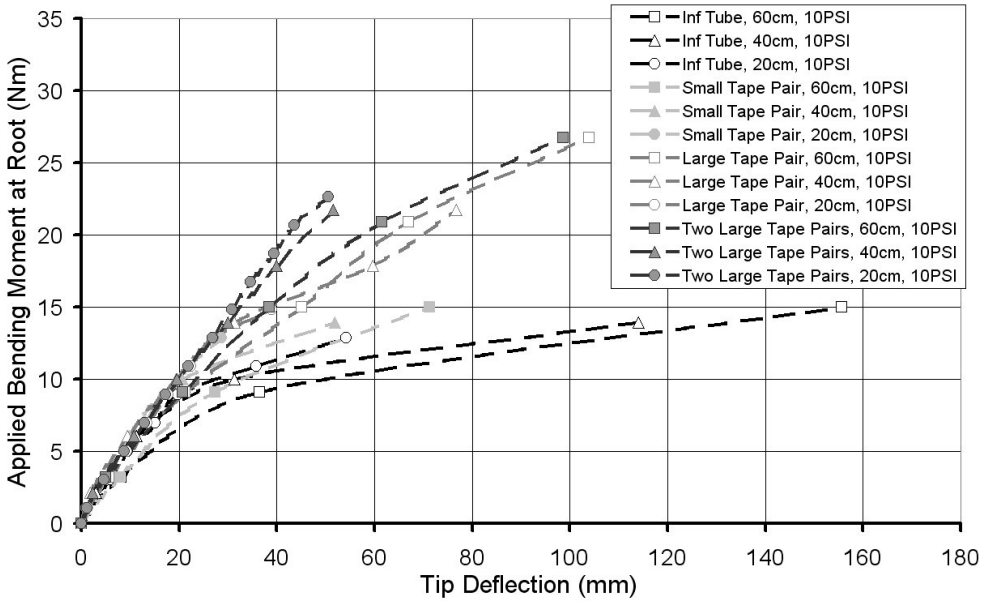

Figure 13: Applied root bending moment against tip deflection for all configurations at 10PSI

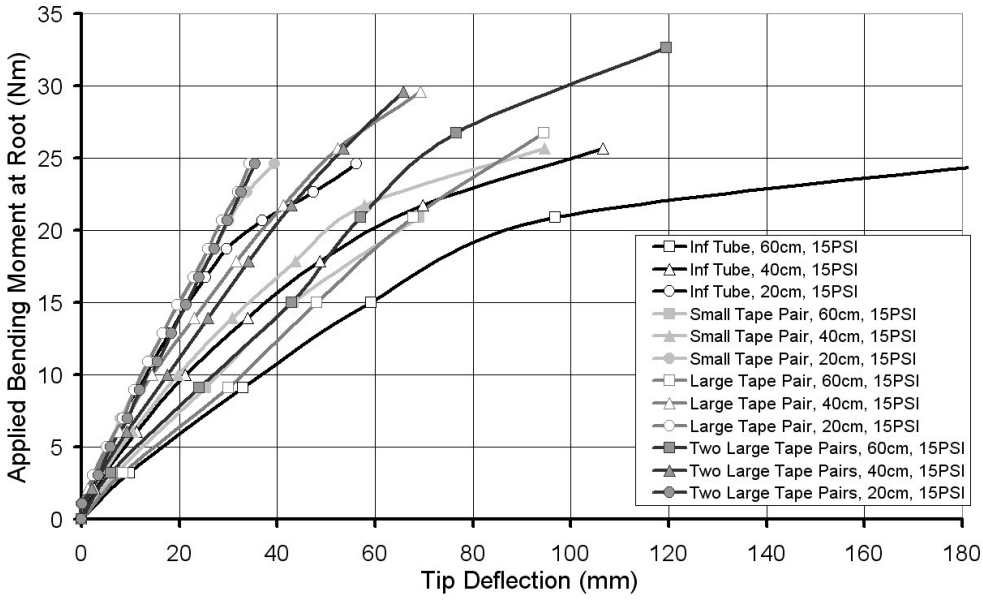

Figure 14: Applied root bending moment against tip deflection for all configurations at 15PSI